Species Specificity of Amidine-Based Urokinase Inhibitors

Vered Klinghofer,*[,‡,§] Kent Stewart,[§,||] Tom McGonigal,[‡] Richard Smith,[||] Aparna Sarthy,[‡] Vicki Nienaber,[||] Chris Butler,[‡] Sarah Dorwin,[||] Paul Richardson,[||] Moshe Weitzberg,[‡] Mike Wendt,[‡] Todd Rockway,[‡] Xumiao Zhao,[‡] Keren I. Hulkower,[‡] and Vincent L. Giranda[‡]

Departments of Cancer Research and Advanced Technology, Abbott Laboratories, Abbott Park, Illinois 60064-6117

Received January 29, 2001; Revised Manuscript Received May 17, 2001

ABSTRACT: Inhibition of the proteolytic activity of urokinase has been shown to inhibit the progression of tumors in rodent models and is being investigated for use in human disease. Understanding the rodent/human species-specificity of urokinase inhibitors is therefore critical for interpretation of rodent cancer progression models that use these inhibitors. We report here studies with a panel of 11 diverse urokinase inhibitors in both human and mouse enzymatic assays. Inhibitors such as amiloride, B428, and naphthamidine, that occupy only the S1 subsite pocket were found to be nearly equipotent between the human and the murine enzymes. Inhibitors that access additional, more distal, pockets were significantly more potent against the human enzyme but there was no corresponding potency increase against the murine enzyme. X-ray crystallographic structures of these compounds bound to the serine protease domain of human urokinase were solved and examined in order to explain the human/mouse potency differences. The differences in inhibitor potency could be attributed to four amino acid residues that differ between murine and human urokinases: 60, 99, 146, and 192. These residues are Asp, His, Ser, and Gln in human and Gln, Tyr, Glu, and Lys in mouse, respectively. Compounds bearing a cationic group that interacts with residue 60 will preferentially bind to the human enzyme because of favorable electrostatic interactions. The hydrogen bonding to residue 192 and steric considerations with residues 99 and 146 also contribute to the species specificity. The nonparallel human/mouse enzyme inhibition observations were extended to a cell-culture assay of urokinase-activated plasminogen-mediated fibronectin degradation with analogous results. These studies will aid the interpretation of in vivo evaluation of urokinase inhibitors.

Urokinase (urokinase type plasminogen activator, uPA) is a trypsin-like serine protease that is important in tissue remodeling. A primary activity of urokinase is the activation of plasminogen which then leads to the breakdown of basement membranes and interstitial matrixes. The activity of urokinase in affecting tissue remodeling has been implicated in a number of disease processes including cancer (reviewed in refs *1*−*4*), atherosclerosis (*5*−*8*), vascular restenosis (*9*, *10*), arthritis (*11*−*14*), postinfarction cardiac rupture (*15*), and macular degeneration (*16*).

The link between urokinase activity and cancer has been widely studied where it is implicated in the invasion and spread of many solid tumors. Compared with normal tissue, many tumors have elevated urokinase activity; furthermore, patients with tumors that have elevated urokinase activity tend to have poorer prognoses (recently reviewed in ref *17*). Experimentally, transgenic animals deficient in urokinase show slowed progression of induced tumors (*18*). Likewise, plasminogen-deficient animals also show slowed progression of tumors (*19*). A number of laboratories have demonstrated modest tumor inhibitory effects of pharmacological inhibitors of urokinase (*20*−*25*).

Urokinase binds to a cellular receptor through its N-terminal growth factor-like domain. Expression of the urokinase receptor is elevated in many cancers where it focuses urokinase activity to the leading edge of an invading tumor (reviewed in refs *1* and *26*). Urokinase may be derived from either the tumor cells or from the surrounding stroma and its origin appears to depend on the tumor type. In colon and breast tumors, the urokinase appears to be predominantly derived from the surrounding stroma (*27*−*30*). Conversely, in squamous cell skin tumors, nonsmall cell lung tumors and glioblastomas the urokinase is substantially derived from the tumor cells (*31*−*37*).

Caution is required when interpreting the results of xenograft experiments that study the role of urokinase or its receptor on tumor progression. Although murine and human urokinases are highly homologous, murine urokinase binds poorly to the human receptor (*38*, *39*). The human urokinase activates human and murine plasminogen more efficiently than does murine urokinase (*40*). Both human and murine urokinases and urokinase receptors are expressed in some xenograft models (*41*). These species differences can potentially confound the interpretation of xenograft models of tumor progression.

* To whom correspondence should be addressed. E-mail: vered.klinghofer@abbott.com. Phone: (847) 937-3892. Fax: (847) 938-2365.

[‡] Department of Cancer Research.

[§] These two authors contributed equally to this work.

[||] Department of Advanced Technology.

10.1021/bi010186u CCC: $20.00
Published on Web 07/14/2001

Table 1: Crystallographic Data Collection and Refinement Statistics

compd	resolution (A)	completenes (final shell)	R_{merge}[a]	$R_{factor}(R_{free})$[b]
1	2.20	99.8 (99.8)	0.108	21.5 (29.1)
2	2.00	89.9 (88.4)	0.083	20.9 (27.7)
3	2.20	93.2 (96.7)	0.062	20.6 (29.9)
4	1.60	97.9 (97.7)	0.073	23.6 (21.0)
5	1.64	95.0 (97.8)	0.139	26.5 (21.1)
7	1.85	96.5 (94.4)	0.050	22.2 (28.4)
8	1.84	97.9 (99.0)	0.138	20.5 (24.4)
9	2.00	96.3 (93.0)	0.139	26.6 (21.0)
11	1.60	87.9 (85.9)	0.065	20.7 (27.5)

[a] $R_{merge} = \sum((I - \langle I \rangle)^2)/\sum(I^2)$. [b] $R_{factor} = [\sum|F_o - F_c|/\sum|F_o|] \times 100$, R_{free} is determined from 10% of the data randomly removed from the refinement.

We have used a structure-based approach to design a series of aryl-amidine based urokinase inhibitors in order to affect the progression of cancers (*42*). These compounds have been optimized to inhibit human urokinase. The compounds bind in the S_1 specificity subsite of urokinase. They also bind in the recently described $S_{1\beta}$ pocket, as well as across the urokinase substrate-binding groove (*43*). Analysis of the murine and human sequences suggests that there are differences between the two species within their active sites. We have used cloned murine and human urokinases to compare inhibitory characteristics of the naphthamidine-based urokinase inhibitors. The crystal structure of the human urokinase in combination with the sequence of the murine enzyme was then used to understand the differences in inhibitory potency of compounds between species.

MATERIALS AND METHODS

Human Urokinase. Human low molecular weight urokinase (residues 136−411), which lacks the N-terminal growth-factor and kringle domains, was used as supplied by Abbott Laboratories as Abbokinase (*44*). The lyophilized powder was resuspended in water to a urokinase stock solution containing 5% human albumin, 0.5% mannitol and 1% NaCl. This stock solution was aliquoted and kept at −80 °C. Before use, it was diluted 50-fold and used at a final concentration of 2−3 nM enzyme and 50 μg/mL of human albumin. Human high molecular weight urokinase, residues 1−411, was prepared as previously described (*44*). Inhibition results shown in Table 2 use Abbokinase. Experiments with high molecular weight urokinase were identical within experimental error (data not shown), consistent with previous results demonstrating independence of the catalytic domain from growth factor and kringle domains (*45*).

Murine Urokinase: Cloning and Expression. Plasmid pdEMP-75 contains the murine urokinase gene derived from a murine kidney cDNA library (GenBank, X02389). To facilitate cloning into a number of different expression vectors, the following PCR primers were synthesized: 5′-GTGTGGATCCATGAAGTCTGGCTGGCGAGCCTG-3′ and 5′-GTGTAGATCTCCCGGGCCATCAGAAGGCCA-GACC-3′. The PCR reactions were performed using the Takara ExTaq PCR kit (Panvera Corp. Madison, WI). PCR was performed with 25 cycles of 94 °C for 30 s, 55 °C for 1 min, and 72 °C for 2 min. The PCR product was then cloned into pGEM-T vector (Promega Madison, WI) to create pAB60, and the sequence was verified. A 1.3 kb *Bam*HI, *Not*I fragment was ligated into *Bam*HI, *Not*I cut pAcMP3 (Pharmingen, San Diego, CA) to create pAB61. All methods for use of the Baculogold expression system including cell culture and virus propagation were performed as described by the manufacturer (Pharmingen). All transfer vectors and viral nucleic acids were obtained from Pharmingen. Grace's supplemented insect media and SF900II media were obtained from Life Technologies (Gaithersburg, MD). Sf9 insect cells were cotransfected with Baculogold viral DNA and pAB61 to generate recombinant virus. For expression of the murine urokinase protein, insect cells were infected at a multiplicity of infection of 5−10. Media containing the secreted protein were collected after 48 h post infection.

Murine Urokinase: Purification and Activation:. Full-length murine pro-urokinase, residues 1−413, was over-expressed in baculovirus SF9 cell cultures. All purification steps were at 4 °C unless otherwise indicated. An S-Sepharose Fast Flow (Amersham Pharmacia, Piscataway, NJ) column (5 × 2.5 cm) was equilibrated in 10 mM MES (Sigma, St. Louis, MO), pH 5.6. Conditioned media, 1.2 L, was diluted with an equal volume of equilibration buffer and applied to the column at 20 mL/min. After washing to baseline, the bound pro-urokinase was eluted in minimal volume by changing directly to 25 mM Tris, 0.5 M NaCl, pH 7.4. Fractions (4 mL each) were pooled according to activity using a microtiter plate assay based on hydrolysis of a chromogenic *p*-nitroanilide substrate S-2444 [DiaPharma Group, Inc. Franklin, OH (*46*)]. The pro-urokinase in the pooled fractions was subsequently converted to active urokinase during a 2-h incubation at 37 °C with biotinylated plasmin. Plasmin had been previously biotinylated using sulfo-NHS-biotin (Pierce, Rockford, IL) following the manufacturer's recommendations. The pro-urokinase activation step was stopped by adding 1 mL of streptavidin-agarose resin (Pierce) to the 67 mL incubation mixture and filtration. The activation incubate was applied to a 25 mL bed *p*-aminobenzamidine column (Sigma) previously equilibrated with buffer B to capture the active murine urokinase. Elution with 500 mM sodium chloride and 100 mM sodium acetate, pH 4.5, yielded fractions containing highly purified murine urokinase.

Human and Murine Urokinase Enzymatic Assays. Human urokinase was used at 2−3nM and murine urokinase was used at 52 nM for inhibitor assays. For compounds potent against murine urokinase (compounds 2, 9, 10) the murine enzyme concentration was lowered to 5.2 nM to ensure that the enzyme concentration was less than the inhibitor concentration during the assay. Both enzymes contain albumin: human albumin with the Abbokinase and bovine albumin with the murine urokinase. The final concentration of albumin in both assays was 50μg/mL. The assay was performed in a 96 well polystyrene, flat bottom plate in a 50 mM Tris/0.15 M NaCl/0.5% Pluronic F-68 (Sigma), pH 7.4 buffer. The compounds were dissolved in DMSO[1] and tested at concentrations of 0.01−250 μM in a final reaction volume of 200 μL. The reactions were initiated by the

[1] Abbreviations: pyroGlu-Gly-Arg-pNA-HCl, L-pyroglutamyl-glycine-arginine *p*-nitroanilide; DMSO, dimethyl sulfoxide; PBS, phosphate buffered saline; Glu-Gly-Arg-CMK, glutamyl-glycine-arginine chloromethyl ketone.

Table 2: Chemical Structures and Assay Results for Human and Murine Urokinases

Compound Number	Structure	K_i (μM) (human)	K_i (μM) (mouse)	K_i ratio mouse/human
1	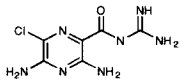	2.8	1.7	0.61
2	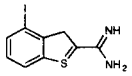	0.10	0.082	0.82
3	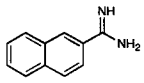	5.9	6.0	1.0
4	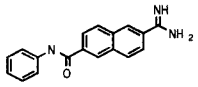	0.63	2.3	3.6
5	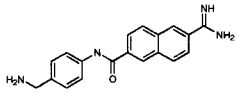	0.040	2	50
6	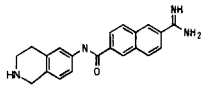	0.016	2.8	170
7	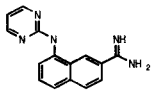	0.035	0.43	12
8	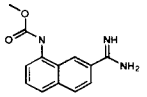	0.040	0.31	7.8
9	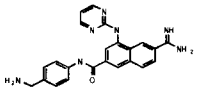	0.00064	0.13	203
10	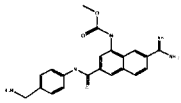	0.00092	0.11	120
11	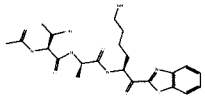	0.048	0.90	19

addition of substrate to a final concentration of 200 μM with human urokinase and 1.5 mM with murine urokinase. The reaction was followed by the formation of *p*-nitroanaline at 405 nm at ambient temperature on a Spectromax (Molecular Devices, Sunnyvale, CA) plate reader for 15 min. K_i values were calculated using the previously established K_m values for S-2444: 55 μM and 1.5 mM for human and murine urokinase, respectively.

Human and Murine Fibronectin Degradation Assays. A modified procedure of Towle et al. (*25*) was used to measure the cell-surface urokinase-mediated activation of plasminogen and subsequent plasmin-mediated degradation of fibronectin. Microtiter plates were precoated with 50 μL/well of 20 μg/mL human fibronectin in 0.1 M sodium phosphate buffer, adjusted to 0.073 μCi with *N*-methyl [^{3}H]human fibronectin (Amersham Pharmacia). After 16−20 h at 37 °C/5% CO_2, the plates were washed three times with sterile PBS (Life Technologies) and incubated covered at 4 °C until use. Both human and murine cells were used in this assay. MiaPaCa-2 (ATCC; human pancreatic carcinoma cells) and Lewis Lung Carcinoma cells (ATCC; murine lung carcinoma) were grown to confluency, washed with sterile PBS, and harvested with Versene (Life Technologies). The cells were resuspended in serum-free media containing 1% BSA at 1×10^6 cells/mL. MiaPaCa-2 or Lewis Lung Carcinoma cells (50 000 cells in 50 μL) were added to the fibronectin coated plates. Serial dilutions of compounds were added as a DMSO/PBS solution so that the final concentration of DMSO was 0.1%. Human plasminogen (Sigma) (0.0215 mg/mL final concentration) was added to each well to start the reaction. The plates were then incubated for 2.5 h at 37 °C/5% CO_2. An aliquot of the reaction mixture (50 μL) was then transferred to a 96-well counting tray containing 200 μL Optiphase scintillation cocktail (Millipore, Bedford, MA). The trays were then counted in a MicroBeta 1450 scintillation counter (Wallac) to quantify the released [^{3}H]fibronectin fragments. Controls included cell-free incubations with and without human plasmin (100 μg/mL; Enzyme Research Labs, South

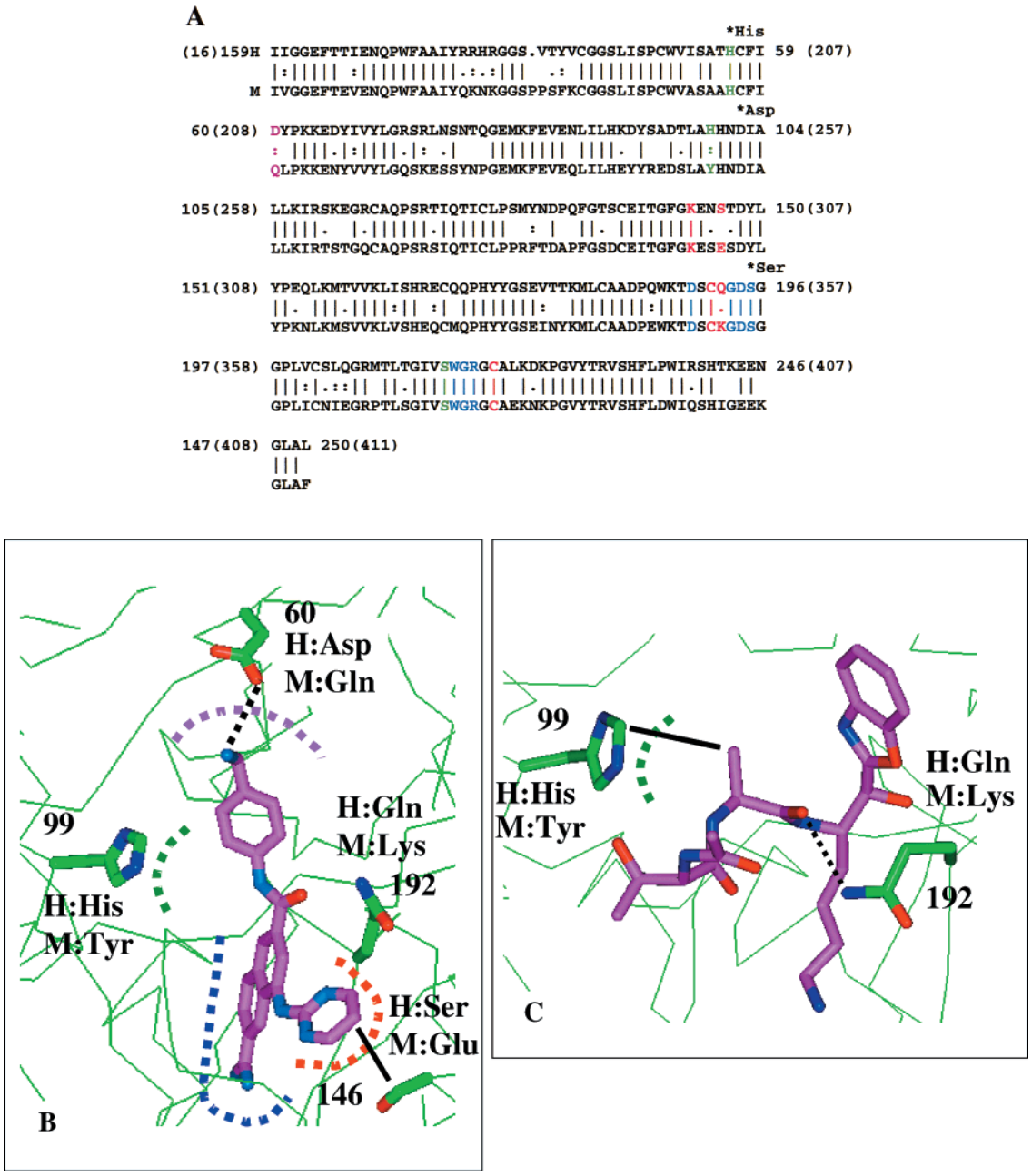

FIGURE 1: (A) Sequence alignment of the protease domain of human (GenBank Q15844, H) and murine (GenBank Q02389, M) urokinases. Chymotrypsinogen numbering is shown with the corresponding human urokinase numbering given in parentheses. The active site triad residues, His 57, Asp 102, and Ser 195 are marked with asterisks. Residues comprising S_1, $S_{1\beta}$, S_2, or Asp sites are color coded (blue, red, green, and magenta, respectively) (B) Protein X-ray crystal structure of compound **9** in the active site of urokinase showing the location of residues which differ between human and murine enzymes. A good hydrogen bond between the inhibitor and Asp 60 is shown as a black dotted line. A good van der Waals contact between the inhibitor and Ser 146 is shown as a black solid line. Dashed lines show the approximate location of the S_1, $S_{1\beta}$, S_2, and Asp sites with color scheme as above. (C) Protein X-ray crystal structure of compound **11** in the active site of urokinase showing the location of contacting residues which differ between human and murine enzymes. A good hydrogen bond between the inhibitor and Gln 192 is shown as a black dotted line. A good van der Waals contact between the inhibitor and His 99 is shown as a black solid line.

Bend, IN) to define the total amount of releasable activity and background release of radioactivity from the well, respectively.

Urokinase Inhibitor Crystal Structures. Amiloride, **1**, was purchased from Sigma. B428, **2**, and naphthamidine, **3**, were synthesized according to literature procedures (*24*, *47*). Compounds **4**−**10** were synthesized at Abbott Laboratories (*48*). The synthesis of compound **11** will be described in a separate publication. Protein X-ray crystallographic studies of the compounds bound to the active site of human urokinase were solved using procedures previously described (*42*, *43*). Briefly, compounds were soaked into existing crystals, and data were collected at 160 K. Data were processed using the HKL program suite (*49*) and refined using the program XPLOR (*50*). Electron density maps were examined using the program QUANTA. Ordered waters were placed in $F_o - F_c$ map peaks greater than 4σ, with good hydrogen bonding geometry. Data collection and refinement statistics for the compounds in Table 2 are shown in Table 1. Coordinates for compounds 1−5, 7−9, and 11 bound to

Table 3: Potencies for Urokinase Inhibitors in Cell-Based Assays

Compound Number	Structure	IC_{50} (μM) MiaPaCa (human)	Lewis Lung (mouse)	IC_{50} ratio mouse/human
2	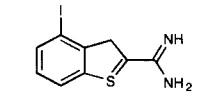	1.4	3.1	2.2
6	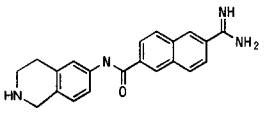	0.26	>10	>38
7	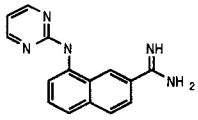	1.0	7.6	7.6
9	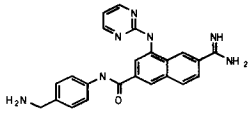	0.0040	0.75	190
11	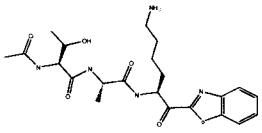	0.22	2.9	13

human urokinase have been deposited with Protein Data Bank.

RESULTS AND DISCUSSION

An alignment of the protease domains of the murine and human enzymes is shown in Figure 1A and indicates an overall identity of 71%. The availability of the protein X-ray structure of the human enzyme allowed us to identify the residues located at the active site that differ between the two species. The sequence alignment in Figure 1A was unambiguous in all regions, except for a single residue deletion at position 38 (Figure 1A) which is far removed from the inhibitor binding region. Thus only side-chain replacements, rather than backbone movement, will characterize the differences between the murine and human enzymes. We have defined the active site as those residues that lie within 6 Å of the peptide inhibitor Glu-Gly-Arg-CMK as observed crystallographically (*51*). The active sites of the urokinase enzymes from the two species have four residue differences between them. These are illustrated in Figure 1B using the crystal structure of compound **9** bound to human urokinase. None of the variable residues reside in the S_1 pocket, but there are potentially important residue differences at more distal regions.

Given this difference in active sites between the murine and human enzymes, we therefore evaluated a structurally diverse set of enzyme inhibitors in both enzymatic and cell-based assays of human and murine urokinases (Table 2 and Table 3, respectively). Compounds **1**, **2**, and **3** are standard benchmark inhibitors of urokinase that have been reported previously (*52*). Amiloride, compound **1**, is an inhibitor of the acylguanidine class, and B428 and naphthamidine, compounds **2** and **3**, respectively, are members of the arylamidine class of enzyme inhibitors. Crystal structures of all three inhibitors showing their orientation within the S_1 subsite have been described (*42*, *53*, *54*). As indicated above, the S_1 subsite possesses no residues that differ between human and murine urokinases. In accord with this fact is the observation of nearly unitary murine/human inhibition K_i ratios (see Table 2).

Compounds **4**−**10** are naphthamidine-class inhibitors that emerged from our urokinase inhibition program (*43*, *48*). They differ from compounds **1**−**3** in having structural extensions that enhance their enzyme inhibition potencies against the human enzyme. Crystal structures of each compound bound to urokinase have been determined, and the active site orientation of compound **9** is shown in Figure 1B and is representative of the series of compounds. Compound **4** gains potency against the human enzyme due to an aryl−aryl interaction with His 57, a member of the catalytic triad of serine proteases. This interaction would be expected to be similar for both human and murine enzymes, and accordingly, the murine/human ratio is not significantly different from naphthamidine.

Compound **5** gains 14-fold in potency against the human enzyme, relative to compound **4**, because of an attractive electrostatic interaction between the positively charged primary amine of the inhibitor and the negatively charged side-chain carboxylate of Asp60 of the human enzyme. This interaction in shown in Figure 1B for compound **9**, and the analogous interaction also occurs for compound **5**. The corresponding protein residue at position 60 in the murine enzyme is Gln, and the interaction would be expected to be weaker due to the lack of charge of the Gln residue.

Cyclization of the benzylamine in compound **5** yields compound **6**. The crystal structures of compounds **5** and **6** indicate similar interactions between their primary or secondary amino groups (respectively) and the Asp 60 of the human urokinase. Accordingly, the murine/human K_i ratio of compounds **5** and **6** are similar.

Compound **7** gains 170-fold in potency against the human enzyme, relative to compound **3**, because of the efficient occupation of the $S_{1\beta}$ hydrophobic exosite pocket by an aminopyrimidine substituent (*43*). This interaction is shown in Figure 1B for compound **9**, and the analogous interaction also occurs for compound **7**. One residue that comprises this $S_{1\beta}$ pocket in the human enzyme is Ser 146, which is replaced by Glu in the murine enzyme. The proximity of the aminopyrimidine unit to residue 146 is illustrated in Figure 1B. While the details of the interaction of the aminopyrimidine of compound **7** with the $S_{1\beta}$ pocket of murine urokinase await crystallographic analysis, the replacement of a neutral Ser with a charged Glu residue suggests that interaction of compound **7** within the murine $S_{1\beta}$ pocket will be significantly altered, relative to the human pocket. The aminopyrimidine substituent leads to a potency gain against the mouse enzyme; however, the difference is only 14-fold relative to compound **3**. Similar results have been demonstrated with compound **8**.

The doubly substituted naphthamidine, compound **9**, possesses the combined structural features of both compounds **5** and **7**, with interactions with both Asp60 and the $S_{1\beta}$ pocket of the human enzyme (Figure 1B) These potency-increasing interactions are additive and lead to sub-nanomolar potency against the human enzyme and a 10000-fold gain in potency relative to the parent naphthamidine compound **3**. In contrast to this very large potency gain against the human enzyme is the observation of only a 70-fold gain in potency of compound **9** against the murine enzyme, relative to compound **3**. The structural explanation for this nonparallel potency enhancement against the human and murine enzymes lies in the summed combination of the structural effects described above for compounds **5** and **7**.

To extend our observations beyond aryl−amidine-based inhibitors of urokinase, compounds **1**−**10**, we evaluated one example of a peptide-mimetic covalent inhibitor. Compound **11** in Table 2 is an Ac−Thr-Ala-Lys-ketobenzoxazole tripeptide inhibitor of urokinase and represents a standard extension of the peptide aldehyde inhibitors reported recently for human urokinase (*55*). This peptide mimetic inhibitor exhibits an apparent K_i of 48 nM against human urokinase and 900 nM against the murine enzyme (19-fold difference).

The binding mode of compound **11** is typical of that found in other peptide-ketobenzoxazole-seine protease complexes (Figure 1C) where the ketobenzoxazole unit makes both hydrogen bonding and van der Waals interactions with Gln 192 of human urokinase. (*56*). In murine urokinase, residue 192 is a Lys, and the specific interactions would be expected to be altered from that observed in human urokinase. In addition to the contacts at residue 192, residue 99 is a His in human urokinase and is part of the S_2 binding pocket. In murine urokinase, residue 99 is Tyr, and this larger residue alters the shape of the binding pocket and decreases the binding affinity of compound **11**.

We measured the activation of plasminogen and subsequent degradation of fibronectin in a cell-based assay. Cells from human (MiaPaCa-2) and murine (Lewis Lung Carcinoma) origin, and hence their cognate urokinase enzymes were tested. The results (Table 3) found in the cellular assay paralleled those seen in the enzymatic assay. Typically, the IC_{50} value for inhibition by a given compound in the cell-based assay is larger than its K_i determined in the enzymatic assay. For those compounds where solubility allowed an accurate determination, the ratios between the murine and human IC_{50} values are very similar to those seen for K_i values in the enzymatic assay (Table 2).

CONCLUSIONS

In summary, 11 urokinase inhibitors from three inhibitor classes, acylguanidine, arylamidine, and peptide-mimetic, with potencies ranging 4 orders of magnitude from 0.6 nM to 6.0 μM against the human enzyme were evaluated. Assays of inhibitory potency in isolated enzyme and in cell systems were carried out. Compounds that occupy only the S_1 subsite contact only amino acid residues that are identical between human and murine urokinases and consequently show no species differences. Compounds that extend beyond the S_1 subsite and achieve potency gains by making additional interactions with four residues that vary between human and murine urokinase, positions 60, 99, 146, and 192, show species-specific affinities. The compounds illustrated here emerged from a discovery effort focused on the human enzyme and exhibit potent inhibitory activity against human urokinase—for example, subnanomolar K_i in the case of compound **9**. The potencies against the murine enzymes are either equal or diminished, relative to the human potencies, and the most potent murine urokinase inhibitor described here has K_i of 85 nM (compound **9**).

Because both murine and human components of the urokinase/urokinase receptor system are expressed in xenograft tumor model systems, caution must be observed when using these systems. Our studies described here will aid with the interpretation and design of in vivo studies of urokinase inhibitors.

ACKNOWLEDGMENT

We thank Anne Rueter for growing the cells used in preparing murine urokinase protein. We also thank Jack Henkin, Don Davidson, Jieyi Wang, and Pat Marcotte for helpful discussions.

REFERENCES

1. Andreasen, P. A., Kjoller, L., Christensen, L., and Duffy, M. J. (1997) *Int. J. Cancer 72*, 1−22.
2. Blasi, F. (1999) *Thromb. Haemost. 82*, 298−304.
3. Dano, K., Romer, J., Nielsen, B. S., Bjorn, S., Pyke, C., Rygaard, J., and Lund, L. R. (1999) *Apmis 107*, 120−7.
4. Johnsen, M., Lund, L. R., Romer, J., Almholt, K., and Dano, K. (1998) *Curr. Opin. Cell Biol. 10*, 667−71.
5. Carmeliet, P., Moons, L., Lijnen, R., Baes, M., Lemaitre, V., Tipping, P., Drew, A., Eeckhout, Y., Shapiro, S., Lupu, F., and Collen, D. (1997) *Nature Genetics 17*, 439−44.
6. Falkenberg, M., Giglio, D., Bjornheden, T., Nygren, H., and Risberg, B. (1998) *J. Vasc. Res. 35*, 318−24.
7. Lupu, F., Heim, D. A., Bachmann, F., Hurni, M., Kakkar, V. V., and Kruithof, E. K. (1995) *Arterioscler., Thromb., Vasc. Biol. 15*, 1444−55.
8. Noda-Heiny, H., Daugherty, A., and Sobel, B. E. (1995) *Arterioscler., Thromb., Vasc. Biol. 15*, 37−43.

9. Christ, G., Kostner, K., Zehetgruber, M., Binder, B. R., Gulba, D., and Huber, K. (1999) *J. Thromb. Thrombolysis 7*, 277−85.
10. Kanse, S. M., Benzakour, O., Kanthou, C., Kost, C., Lijnen, H. R., and Preissner, K. T. (1997) *Arterioscler., Thromb., Vasc. Biol. 17*, 2848−54.
11. Del Rosso, M., Fibbi, G., and Matucci Cerinic, M. (1999) *Clin. Exp. Rheumatol. 17*, 485−98.
12. Busso, N., Peclat, V., Van Ness, K., Kolodzieszyk, E., Degen, J., Bugge, T., and So, A. (1998) *J. Clin. Invest. 102*, 41−50.
13. Medcalf, R. L., and Hamilton, J. A. (1986) *Arthritis Rheum. 29*, 1397−401.
14. Koolwijk, P., Miltenburg, A. M., van Erck, M. G., Oudshoorn, M., Niedbala, M. J., Breedveld, F. C., and van Hinsbergh, V. W. (1995) *J. Rheumatol. 22*, 385−93.
15. Heymans, S., Luttun, A., Nuyens, D., Theilmeier, G., Creemers, E., Moons, L., Dyspersin, G. D., Cleutjens, J. P., Shipley, M., Angellilo, A., Levi, M., Nube, O., Baker, A., Keshet, E., Lupu, F., Herbert, J. M., Smits, J. F., Shapiro, S. D., Baes, M., Borgers, M., Collen, D., Daemen, M. J., and Carmeliet, P. (1999) *Nat. Med. 5*, 1135−42.
16. Das, A., McGuire, P. G., Eriqat, C., Ober, R. R., DeJuan, E., Jr., Williams, G. A., McLamore, A., Biswas, J., and Johnson, D. W. (1999) *Invest.Ophthalmol. Vis. Sci. 40*, 809−13.
17. Duffy, M. J., Maguire, T. M., McDermott, E. W., and O'Higgins, N. (1999) *J. Surg. Oncol. 71*, 130−5.
18. Shapiro, R. L., Duquette, J. G., Roses, D. F., Nunes, I., Harris, M. N., Kamino, H., Wilson, E. L., and Rifkin, D. B. (1996) *Cancer Res. 56*, 3597−604.
19. Bugge, T. H., Lund, L. R., Kombrinck, K. K., Nielsen, B. S., Holmback, K., Drew, A. F., Flick, M. J., Witte, D. P., Dano, K., and Degen, J. L. (1998) *Oncogene 16*, 3097−104.
20. Xing, R. H., Mazar, A., Henkin, J., and Rabbani, S. A. (1997) *Cancer Res. 57*, 3585−93.
21. Rabbani, S. A., Harakidas, P., Davidson, D. J., Henkin, J., and Mazar, A. P. (1995) *Int. J. Cancer 63*, 840−5.
22. Alonso, D. F., Farias, E. F., Ladeda, V., Davel, L., Puricelli, L., and Bal de Kier Joffe, E. (1996) *Breast Cancer Res. Treat. 40*, 209−23.
23. Alonso, D. F., Tejera, A. M., Farias, E. F., Bal de Kier Joffe, E., and Gomez, D. E. (1998) *Anticancer Res. 18*, 4499−504.
24. Bridges, A. J., Lee, A., Schwartz, C. E., Towle, M. J., and Littlefield, B. A. (1993) *Bioorg. Med. Chem. 1*, 403−10.
25. Towle, M. J., Lee, A., Maduakor, E. C., Schwartz, C. E., Bridges, A. J., and Littlefield, B. A. (1993) *Cancer Res. 53*, 2553−9.
26. Mondino, A., Resnati, M., and Blasi, F. (1999) *Thromb. Haemostasis 82*, 19−22.
27. Pyke, C., Kristensen, P., Ralfkiaer, E., Grondahl-Hansen, J., Eriksen, J., Blasi, F., and Dano, K. (1991) *Am. J. Pathol. 138*, 1059−67.
28. Christensen, L., Wiborg Simonsen, A. C., Heegaard, C. W., Moestrup, S. K., Andersen, J. A., and Andreasen, P. A. (1996) *Int. J. Cancer 66*, 441−52.
29. Nielsen, B. S., Sehested, M., Timshel, S., Pyke, C., and Dano, K. (1996) *Laboratory Invest. 74*, 168−77.
30. Pyke, C., Graem, N., Ralfkiaer, E., Ronne, E., Hoyer-Hansen, G., Brunner, N., and Dano, K. (1993) *Cancer Res. 53*, 1911−5.
31. Parolini, S., Flagiello, D., Cinquetti, A., Gozzi, R., Cristini, S., Cappiello, J., Nicolai, P., Rusnati, M., Presta, M., and Tosatti, M. M. (1996) *Br. J. Cancer 74*, 1168−74.
32. Sandstrom, M., Johansson, M., Sandstrom, J., Bergenheim, A. T., and Henriksson, R. (1999) *Int. J. Dev. Neurosci. 17*, 473−81.
33. Morita, S., Sato, A., Hayakawa, H., Ihara, H., Urano, T., Takada, Y., and Takada, A. (1998) *Int. J. Cancer 78*, 286−92.
34. Bolon, I., Devouassoux, M., Robert, C., Moro, D., Brambilla, C., and Brambilla, E. (1997) *Am. J. Pathol. 150*, 1619−29.
35. Gladson, C. L., Pijuan-Thompson, V., Olman, M. A., Gillespie, G. Y., and Yacoub, I. Z. (1995) *Am. J. Pathol. 146*, 1150−60.
36. Yamamoto, M., Sawaya, R., Mohanam, S., Bindal, A. K., Bruner, J. M., Oka, K., Rao, V. H., Tomonaga, M., Nicolson, G. L., and Rao, J. S. (1994) *Cancer Res. 54*, 3656−61.
37. Sappino, A. P., Belin, D., Huarte, J., Hirschel-Scholz, S., Saurat, J. H., and Vassalli, J. D. (1991) *J. Clin. Invest. 88*, 1073−9.
38. Quax, P. H., Grimbergen, J. M., Lansink, M., Bakker, A. H., Blatter, M. C., Belin, D., van Hinsbergh, V. W., and Verheijen, J. H. (1998) *Arterioscler., Thromb., Vasc. Biol. 18*, 693−701.
39. Estreicher, A., Wohlwend, A., Belin, D., Schleuning, W. D., and Vassalli, J. D. (1989) *J. Biol. Chem. 264*, 1180−9.
40. Lijnen, H. R., Van Hoef, B., and Collen, D. (1996) *Eur. J. Biochem. 241*, 840−8.
41. Romer, J., Pyke, C., Lund, L. R., Eriksen, J., Kristensen, P., Ronne, E., Hoyer-Hansen, G., Dano, K., and Brunner, N. (1994) *Int. J. Cancer 57*, 553−60.
42. Nienaber, V., Wang, J., Davidson, D., and Henkin, J. (2000) *J. Biol. Chem. 275*, 7239−48.
43. Nienaber, V. L., Davidson, D., Edalji, R., Giranda, V. L., Klinghofer, V., Henkin, J., Magdalinos, P., Mantei, R., Merrick, S., Severin, J. M., Smith, R. A., Stewart, K., Walter, K., Wang, J., Wendt, M., Weitzberg, M., Zhao, X., and Rockway, T. (2000) *Structure 8*, 553−63.
44. Marcotte, P. A., Henkin, J., Credo, R. B., and Badylak, S. F. (1992) *Fibrinolysis 6*, 69−78.
45. Novokhatny, V., Medved, L., Mazar, A., Marcotte, P., Henkin, J., and Ingham, K. (1992) *J. Biol. Chem. 267*, 3878−85.
46. Huseby, R. M., and Smith, R. E. (1980) *Sem. Thromb. Hemostasis 7*, 175.
47. Geratz, J. D., Shaver, S. R., and Tidwell, R. R. (1981) *Thromb. Res. 24*, 73−83.
48. Geyer, A. G., McClellan, W. J., Rockway, T. W., Stewart, K. D., Weitzberg, M., and Wendt, M. D. (1999) *Urokinase Inhibitors*, World Patent Application 05096.
49. Otwinowski, Z., and Minor, W. (2000) *Methods Enzymol. 276*, 307−26.
50. Brunger, A. T. (1993) *X-PLOR version 3.1 manual*, Yale University Press, New Haven, CT.
51. Spraggon, G., Phillips, C., Nowak, U. K., Ponting, C. P., Saunders, D., Dobson, C. M., Stuart, D. I., and Jones, E. Y. (1995) *Structure 3*, 681−91.
52. Rosenberg, S. (1999) *Annu. Rep. Med. Chem. 34*, 121−28.
53. Zeslawska, E., Schweinitz, A., Karcher, A., Sondermann, P., Sperl, S., Sturzebecher, J., and Jacob, U. (2000) *J. Mol. Biol. 301*, 465−75.
54. Katz, B. A., Mackman, R., Luong, C., Radika, K., Martelli, A., Sprengeler, P. A., Wang, J., Chan, H., and Wong, L. (2000) *Chem. Biol. 7*, 299−312.
55. Tamura, S. Y. (2000) *Bioorg. Med. Chem. Lett. 10*, 983−987.
56. Recacha, R., Carson, M., Costanzo, M. J., Maryanoff, B., DeLucas, L. J., and Chattopadhyay, D. (1999) *Acta Crystallogr., Sect. D 55*, 1785−1791.

BI010186U